Surface Plasmon Resonance Spectroscopy Studies of Membrane Proteins: Transducin Binding and Activation by Rhodopsin Monitored in Thin Membrane Films

Z. Salamon,* Y. Wang,* J.L. Soulages,* M.F. Brown,# and G. Tollin*
Departments of *Biochemistry and #Chemistry, University of Arizona, Tucson, Arizona 85721 USA

ABSTRACT Surface plasmon resonance (SPR) spectroscopy can provide useful information regarding average structural properties of membrane films supported on planar solid substrates. Here we have used SPR spectroscopy for the first time to monitor the binding and activation of G-protein (transducin or G_t) by bovine rhodopsin incorporated into an egg phosphatidylcholine bilayer deposited on a silver film. Rhodopsin incorporation into the membrane, performed by dilution of a detergent solution of the protein, proceeds in a saturable manner. Before photolysis, the SPR data show that G_t binds tightly ($K_{eq} \approx 60$ nM) and with positive cooperativity to rhodopsin in the lipid layer to form a closely packed film. A simple multilayer model yields a calculated average thickness of about 57 Å, in good agreement with the structure of G_t. The data also demonstrate that G_t binding saturates at a G_t/rhodopsin ratio of approximately 0.6. Moreover, upon visible light irradiation, characteristic changes occur in the SPR spectrum, which can be modeled by a 6 Å increase in the average thickness of the lipid/protein film caused by formation of metarhodopsin II (MII). Upon subsequent addition of GTP, further SPR spectral changes are induced. These are interpreted as resulting from dissociation of the α-subunit of G_t, formation of new MII-G_t complexes, and possible conformational changes of G_t as a consequence of complex formation. The above results clearly demonstrate the ability of SPR spectroscopy to monitor interactions among the proteins associated with signal transduction in membrane-bound systems.

INTRODUCTION

Surface plasmon resonance (SPR) spectroscopy is a highly sensitive method for monitoring the properties of biomolecules immobilized on an aqueous metal surface. In the present application of this technology, immobilization is accomplished by incorporation of an integral membrane protein into a planar egg phosphatidylcholine (PC) membrane supported on a thin silver film. Previous work from this laboratory has employed SPR spectroscopy to characterize the structural properties of such solid-supported PC membranes (Salamon et al., 1994b), to investigate the mechanism of binding of an apolipoprotein to a diacylglycerol-containing PC bilayer (Soulages et al., 1995), and to follow the interactions between a photoactive yellow protein and lipid bilayers (Salamon et al., 1995). We have also utilized SPR to detect conformational events occurring during rhodopsin photolysis, using bovine rhodopsin incorporated into a PC membrane (Salamon et al., 1994a). The correspondence between the pH dependencies of the observed SPR changes and those of optical signals obtained with parallel flash photolysis studies (Gibson and Brown, 1993) suggests that the SPR experiment monitors the metarhodopsin I–metarhodopsin II (MI-MII) transition of photolyzed rhodopsin, which we have interpreted in terms of a light-induced protrusion of the protein from the membrane in the MII state (Salamon et al., 1994a). Such a protrusion of rhodopsin from the membrane may be associated with the influences of the membrane lipid environment on the MI-MII transition, particularly the influences of lipids favoring the reverse-hexagonal (HII) phase (Deese et al., 1981; Wiedmann et al., 1988; Gibson and Brown, 1993; Brown, 1994). The driving force for the MI-MII transition may originate from the frustration due to the curvature free energy of the bilayer. In the present experiments, we have extended these studies by utilizing SPR spectroscopy to investigate the interaction between rhodopsin and its associated G-protein transducin.

Heterotrimeric GTP-binding proteins (G-proteins) play a key role as mediators between receptors and effectors in transmembrane signaling pathways (Gilman, 1987; Taylor, 1990; Coleman et al., 1994). Signal transduction is initiated by the coupling of G-proteins to hormonal, neurotransmitter, and sensory receptors. Stimulated receptors cause the release of GDP from the α-subunits of the G-protein (Simon et al., 1991; Dratz et al., 1993); subsequent GTP binding to the α-subunits produces a metastable conformational state, which functions as an information carrier (Gilman, 1987; Bourne et al., 1990, 1991; Simon et al., 1991; Coleman et al., 1994) controlling effectors such as adenylyl cyclases, phosphodiesterases, phospholipases, and ion channels (Simon et al., 1991). Rhodopsin is currently the best characterized of such membrane-bound receptor proteins and serves as a specific paradigm for the superfamily of G-protein-coupled receptors. It is known that most G-proteins are rather tightly anchored to the membrane in both unstimulated and stimulated cells (Gilman, 1987; Hamm, 1991). The G-protein, which interacts with rhodopsin

Received for publication 30 October 1995 and in final form 27 March 1996.

Address reprint requests to Dr. Gordon Tollin, Department of Biochemistry, University of Arizona, Tucson, AZ 85721. Tel.: 520-621-3447; Fax: 520-621-9288; E-mail: tollin@biosci.arizona.edu.

0006-3495/96/07/283/12 $2.00

(transducin or G_t), is peripherally bound to the rod outer segment (ROS) membrane in the dark (for a review, cf. Hargrave and McDowell, 1992) and has been shown to bind to rhodopsin-containing vesicles made from egg phospholipids (PC and PE) (Fung, 1983), suggesting that rhodopsin is the major site of docking of G_t with the membrane. Membrane mixing and light scattering (Hamm et al., 1987; Schleicher and Hofmann, 1987) measurements have variously evaluated the G_t dissociation constant in dark-adapted ROS membranes as 10^{-7} to 10^{-5} M, values that comprise a rather wide range.

After stimulation by green light (498 nm), rhodopsin relaxes within milliseconds to generate an equilibrium mixture of forms, metarhodopsins I and II (Franke et al., 1988; Franke et al., 1990; Kibelbek et al., 1991; Brown, 1994). The formation of MII is dependent on a number of factors, including pH, temperature, and the membrane lipid environment (Wiedmann et al., 1988; Brown and Gibson, 1993; Brown, 1994). It is known that MII interacts with G_t, resulting in binding and activation (Franke et al., 1990; Stryer, 1991), and a concomitant shift of the MI/MII equilibrium to yield "extra MII" (Emeis et al., 1982; Hofmann; 1986; König et al., 1989; Franke et al., 1990; Arnis and Hofmann, 1993; 1995). This extra MII is a stoichiometric measure of the amount of MII-G_t complex formed and can be monitored spectroscopically after a flash of actinic light. The interaction between transducin and photolyzed rhodopsin also leads to a change in the classical Rayleigh light scattering of ROS or disk membrane suspensions (Bennett and Dupont, 1985; Schleicher and Hofmann, 1987). Kinetic measurements clearly indicate that the scattering changes reflect not only binding itself but also the subsequent processes. These include structural alterations in the membrane reflected by either the membrane refractive index or changes in thickness (Michel-Villaz et al., 1984), as well as the relatively slow light-induced shift in the MI/MII equilibrium (i.e., extra MII formation) occurring as a result of photolyzed rhodopsin-transducin complex formation (Schleicher and Hofmann, 1987). Upon photolysis, the affinity of G_t for the MII form of rhodopsin increases to values in the range of 10^{-9} to 10^{-7} M (Bennett and Dupont, 1985).

Three cytoplasmic loops of the MII state of rhodopsin have been shown to interact with three sites on G_t during the binding and activation process (König et al., 1989; Hausdorff et al., 1990; Hamm, 1991; Arnis and Hofmann, 1993; 1995; Dratz et al., 1993). The carboxyl terminus of the α-subunit of G_t is also important for interaction with rhodopsin (Sullivan et al., 1987; Hamm et al., 1988; Weingarten et al., 1990; Sukumar and Higashijma, 1992; Conklin et al., 1993; Dratz et al., 1993). An 11-residue peptide derived from the C-terminus of the α-subunit of G_t binds to MII in the native rod disk membranes (Hofmann, 1986; König et al., 1989) and can also bind to unphotolyzed rhodopsin (Dratz et al., 1993). Conserved leucines and a phenylalanine in this peptide suggest that the receptor binding sites for the G_t α-subunit may be hydrophobic in nature (Dratz et al., 1993). There is also evidence for the importance of hydrophobic residues in two of the three loops of the cytoplasmic domain of rhodopsin, which interacts with G_t (Dixon et al., 1988). It is not known whether conformations of rhodopsin other than MII can activate G_t or regulate the cell's responsiveness. Physiological studies of dark adaptation have suggested that a non-MII conformation, possibly opsin, plays a role in controlling the sensitivity of the cell to light (Corless et al., 1982; Jones et al., 1989; Corson et al., 1990). In this context, a recent biochemical study has clearly demonstrated that bovine opsin is capable of stimulating the exchange of guanyl nucleotides by G_t in a light- and hydroxylamine-insensitive manner (Surya et al., 1994).

Here SPR spectroscopy has been used to obtain additional qualitative and quantitative insights into structure/function relationships involving rhodopsin-containing membranes. Interaction of the G_t with rhodopsin, both before and subsequent to light activation, is detected via characteristic SPR spectral changes that are interpretable in terms of an increase in the average thickness of the membrane film. These results demonstrate that G_t binds strongly and cooperatively to dark-adapted rhodopsin, and that further characteristic changes occur in the SPR spectra upon light activation and subsequent GTP/GDP exchange. Consequently, new knowledge of the binding and structural aspects associated with the interaction of the signal-transducing G protein with rhodopsin is obtained with the use of SPR spectroscopy.

EXPERIMENTAL PROCEDURES

Purification of retinal rod membranes and isolation of transducin

Bovine rod outer segment (ROS) membranes containing rhodopsin were prepared from frozen retinas (Papermaster and Dreyer, 1974) and characterized kinetically as previously described (Gibson and Brown, 1993). The preparations typically had A_{280}/A_{500} absorbance ratios of 2.5, were completely bleached by actinic illumination, and were 99% regenerable with 11-*cis*-retinal. G_t was purified from ROS following published protocols (Kühn, 1980; Fung et al., 1981) and was judged to be at least 90% pure, based on analysis by sodium dodecyl sulfate-polyacrylamide gel electrophoresis (Wessling-Resnick and Johnson, 1987). GTPase activity was assayed according to the procedure of Baehr et al. (1982); a value of 5.8 pmol GTP hydrolyzed μg^{-1} min^{-1} was obtained, in reasonable agreement with values in the literature (Kühn, 1980; Fung et al., 1981).

Preparation of egg PC membrane films on silver substrates

Lipid films were formed on a metallic silver surface from a solution containing 7 mg/ml egg PC in squalene (Fluka)/butanol (0.2:10, v/v), using a procedure originally developed to form freely suspended lipid bilayer membranes separating two aqueous solutions (Mueller et al., 1962). The method, which is based on the interaction between a nascent hydrophilic metallic surface and amphipathic lipid molecules, involves spreading a small amount of lipid bilayer-forming solution (about 2–4 μl) via a Hamilton microsyringe across an orifice in a Teflon sheet (4 mm in diameter) that separates the silver film from the aqueous phase (Salamon et al., 1994b). The hydrophilic surface of the metal attracts the polar groups of the lipid molecules, thus forming an adsorbed lipid monolayer with the

hydrocarbon chains oriented toward the bulk lipid phase. Subsequent to this first step of lipid membrane formation, the main body of the sample cell is filled with the appropriate aqueous solution. This initiates the second step, which involves a thinning process, i.e., formation of both the second monolayer and a Plateau-Gibbs border that anchors the bilayer film to the Teflon spacer, allowing the excess of lipid and solvent to move out of the Teflon orifice. In the present experiments, silver films on a glass prism were prepared by vacuum deposition at the Optical Sciences Center of the University of Arizona, and each metal film was used only one time. Inasmuch as each film has a slightly different thickness, the angle at which resonance occurs in an SPR experiment varies over a range of ±5°, and the spectral shape is also variable (see below).

Preparation of planar supported membrane films containing rhodopsin

All experiments were performed in dim red light (Kodak safelight filter no. 1; 15-W bulb). Rhodopsin was incorporated into a preformed lipid membrane deposited on the surface of the silver film. This was done by adding small aliquots of a concentrated solution of bovine ROS membranes solubilized in 200 mM octyl glucoside to the aqueous compartment of the SPR cell, which contained 10 mM phosphate buffer plus 5 mM Mg acetate at pH 6.0, thereby diluting the detergent to a final concentration below its critical micelle concentration (25 mM) (Salamon et al., 1994a). Based on our previous results, we have used rhodopsin incorporated into a PC bilayer at pH 6.0 to generate sufficient MII to be able to measure G_t binding and activation. After reaching saturation (approximately 6 μM rhodopsin added to the total aqueous phase), small aliquots of a G_t solution in buffer were added to the aqueous compartment of the SPR cell. After the SPR spectral changes that occurred upon the addition of G_t reached a maximum, the sample was flashed with yellow light ($\lambda > 515$ nm), and SPR spectra were measured. Finally, GTP was added to the sample, and SPR spectra were again recorded.

Regeneration of photolyzed rhodopsin with 11-*cis*-retinal

To incorporate retinal as efficiently as possible into a solid-supported lipid bilayer, the typical procedure used to regenerate photolyzed rhodopsin (Wilden and Kühn, 1982) was modified, utilizing the same methodology applied to incorporate rhodopsin into the lipid membrane. The 11-*cis*-retinal was dissolved in 200 mM octyl glucoside, and a small aliquot (15 μl) of the solution was added to the aqueous compartment of the SPR cell containing a preformed lipid bilayer (with or without photolyzed rhodopsin), thereby diluting the detergent by a factor of 100 to a final concentration below its critical micelle concentration. The final retinal concentration added to the aqueous phase was 100 μM. Regeneration was allowed to take place at room temperature ($T = 23 \pm 1$°C) for about 30 min (i.e., until the SPR spectrum stabilized).

PRINCIPLES OF SURFACE PLASMON RESONANCE SPECTROSCOPY APPLIED TO THIN MEMBRANE FILMS

General description

Details of the present procedures for SPR measurement and data analysis have been described elsewhere (Salamon et al., 1994a,b, 1995; Soulages et al., 1995). The method is based upon the resonant excitation by photons from a CW He-Ne laser ($\lambda = 6328$ Å), passing through a glass prism under total internal reflection conditions, of collective electronic oscillations (plasmons) in a thin metal film deposited on the external surface of the prism and in contact with an aqueous compartment (see Fig. 1). The evanescent electromagnetic field thereby generated in the metallic layer can

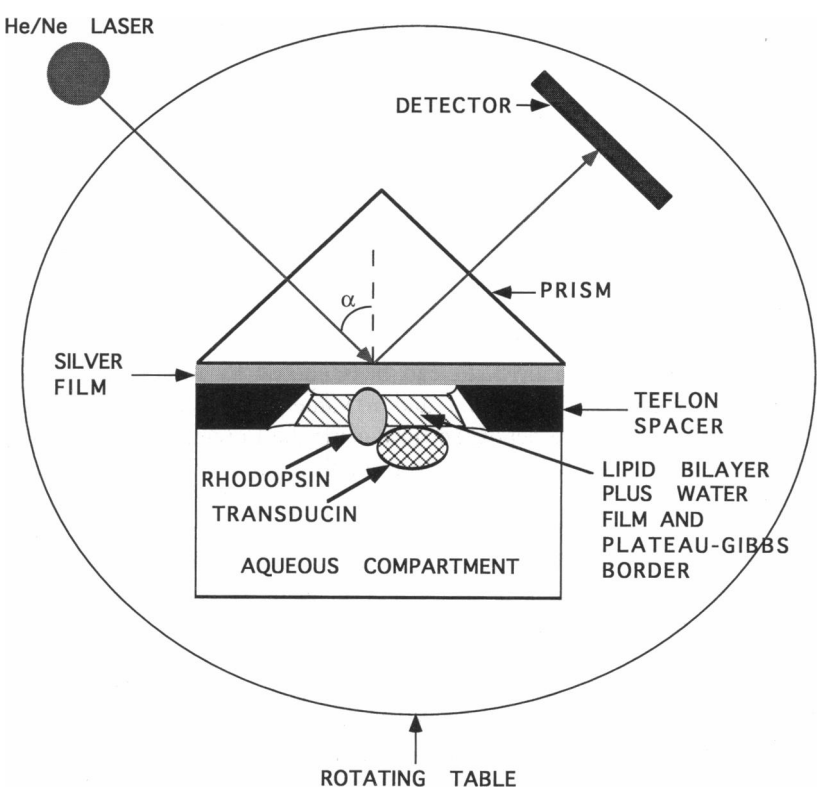

FIGURE 1 A cross-sectional view (from top) of the experimental geometry used for surface plasmon resonance spectroscopic studies of self-assembled lipid bilayer membranes on solid substrates containing membrane-bound proteins interacting with their soluble biochemical partners. The lipid bilayer and its Plateau-Gibbs border are shown in contact with an adsorbed layer of water on the surface of the silver film; also shown are a molecule of rhodopsin incorporated into the lipid layer and a molecule of transducin interacting with it. See text for details.

couple to electronic motions in dielectric materials (such as a proteolipid film) deposited on the front surface of the metal. This situation can be treated by classical electromagnetic theory (cf. Salamon et al., 1994b, for a discussion). In our procedure, the incident angle of the laser beam (α; see Fig. 1; measured with an accuracy of $\pm$ 0.01°) is varied with respect to the back surface of the metal film, and the reflected light intensity is measured.

The theoretical analysis, which allows curve-fitting procedures to be applied to such resonance spectra (i.e., curves of reflectance versus incident angle), utilizes a relationship between reflectance and the optical admittance of the multilayer system (Salamon et al., 1994b). The latter quantity (Y) is defined by the ratio of the amplitudes of the magnetic (B) and electric (C) fields of the electromagnetic wave:

$$Y = C/B. \tag{1}$$

These in turn are described by the following matrix equation, which includes the refractive index n, the film thickness t, the nonresonant absorption coefficient k, and the incident angle α:

$$\begin{bmatrix} B \\ C \end{bmatrix} = \prod_{r=1}^{p} \begin{bmatrix} \cos\delta_r & i(\sin\delta_r)/y_r \\ y_r/\sin\delta_r & \cos\delta_r \end{bmatrix} \begin{bmatrix} 1 \\ y_{r+1} \end{bmatrix} \tag{2}$$

In Eq. 2, $\delta_r = 2(n - ik)_r t_r(\cos\alpha_r)/\lambda$, $y_r = (n - ik)_r/\cos\alpha_r$, and p is the number of dielectric layers deposited on the incident medium (in our case, the medium for which $r = 0$ is a glass prism, whereas $(r + 1)$ is an aqueous solution; see Fig. 1). The reflectance (R) of such a multilayer system is given by the following relationship involving the admittance:

$$R = (y_0 - Y)^2/(y_0 + Y)^2, \tag{3}$$

where y_0 is the admittance of the incident medium (i.e., the glass prism). Equation 3 describes the surface plasmon resonance phenomenon and can be used, via procedures described below, to obtain the optical parameters (n, k, and t) of each of the dielectric layers.

Inasmuch as the incident laser light never reaches the front surface of the metal, light scattering or dispersion effects in the dielectric layer are unimportant (although the evanescent electromagnetic field can be scattered by the dielectric materials). From the t and n values, one can calculate the mass of the deposited film, using the Lorentz-Lorenz equation (see below) for the refractive index of a mixture of buffer, lipid, and protein (Born and Wolf, 1965; Salamon et al., 1994a,b). The method is highly sensitive (approximately 0.06 ng of material deposited per square millimeter of surface can be detected) and is capable of high precision (changes in average thickness of $\pm$ 1 Å can be detected; experimental errors in n and k are estimated to be $\pm$0.02; see below). It is important to emphasize that although the spatial resolution of the structure of the dielectric layer is limited by the wavelength used to measure the resonance, determination of the overall dimensions of the metal plus dielectric films is not, and therefore the latter can be applied to structural measurements with high precision. It should also be noted that effects on n due to anomalous dispersion resulting from rhodopsin photolysis are expected to be at least two orders of magnitude smaller than the above error limits.

In general, two procedures can be used to evaluate the optical parameters of a layer of biological material adsorbed onto the front surface of a silver film using the SPR method: 1) one can obtain SPR spectra as a function of excitation wavelength and analyze them by solving Maxwell's equations (Macleod, 1986; Lopez-Rios and Vuye, 1979); 2) one can obtain an SPR spectrum excited at one wavelength and analyze it by fitting a theoretical resonance curve to the experimental one. The latter technique was first implemented by Kretschmann (Kretschmann, 1971; Haltom et al., 1979) and is based on the principle that a unique set of optical parameters can be evaluated from the surface plasmon reflectance minimum, its depth, and its half-width. The original procedure has been further refined by the application of computer-based optimization methods, which allow a systematic search for a global minimum in the fitting error (Liddell, 1981; Tang and Zheng, 1982; Zhang et al., 1987).

Fitting of experimental SPR curves

In the present application, the Kretschmann procedure has been followed, using a nonlinear least-squares fitting algorithm to define the global minimum. As an example of the application of this methodology, Fig. 2 shows a set of theoretical resonance curves in which the three optical parameters (n, t, and k) are varied. The results illustrate the ways in which these optical parameters influence the shape, the depth, and the position of the resonance minimum of the SPR curve. As a further illustration of the procedures for data reduction, we have also included in Fig. 2 representative error curves for fitting of these three parameters to experimental data obtained from a PC bilayer deposited on a silver film (insets in Fig. 2, *A–C*). It is evident from Fig. 2 *A* that an increase in n shifts the resonance minimum to larger angles, together with an increase the depth of the resonance minimum and an increase in the spectral width. In contrast, Fig. 2 *B* shows that an increase in t decreases the resonance depth, without appreciable change in spectral width, accompanied by a somewhat smaller shift to larger angles. Finally, Fig. 2 *C* shows that the k parameter strongly influences the resonance depth as well as the width, with only a very slight effect on the resonance position. These curves clearly illustrate the fact that the optical parameters are well separated in the theoretical equations describing the plasmon resonance phenomenon (Salamon et al., 1994b), which allows for their independent use during the fitting procedure to arrive at a global minimum. Furthermore, the data presented in the insets demonstrate that the method is capable of high precision in the evaluation of the optical parameters, as has been discussed by Kretschmann (1971) and subsequently by others (Haltom et al., 1979). It follows

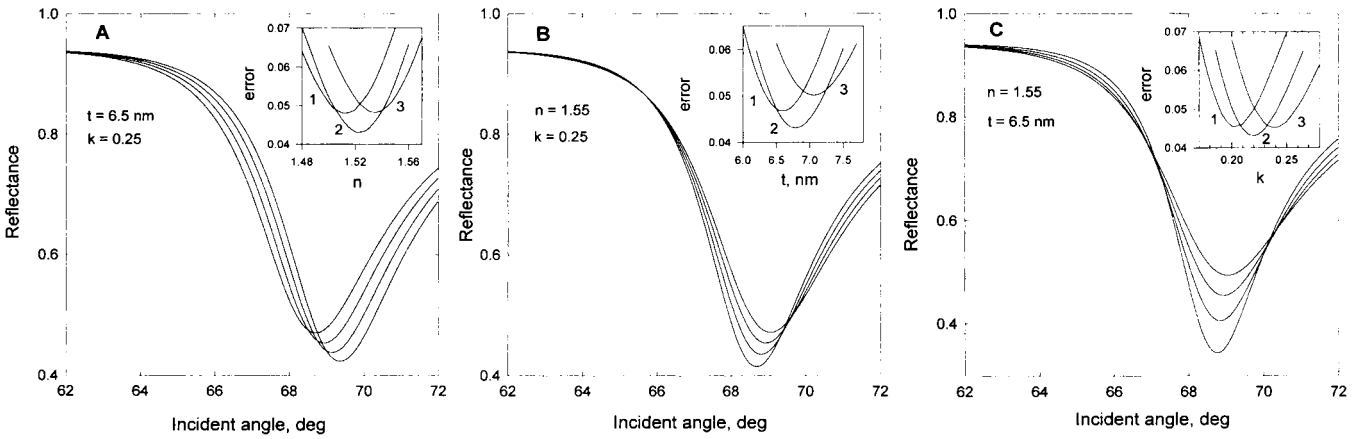

FIGURE 2 Theoretical SPR spectra obtained using a two-layer model (see text for description) for a silver film of 52 nm average thickness coated with a dielectric layer having optical parameters within the range typical of lipid bilayer membranes. The fractional decrease in total reflected light as a function of the incident angle is plotted, showing the sensitivity of the SPR spectra to the various parameter values. Inserts are least-squares error plots obtained from theoretical fits of data for an experimental SPR curve obtained with a PC film deposited on a silver surface (not shown). The best fit parameters to the experimental SPR data are as follows: deposited silver layer: $n = 0.13$; $t = 51.4$ nm; $k = 4.30$ (these values are consistent with those previously published; cf. Schulz and Tangherlini, 1954); PC layer: $n = 1.52$; $t = 6.8$ nm; $k = 0.22$. Error curves were obtained by fixing the parameters for the silver layer, and varying the parameters for the PC layer as indicated in the legend for each panel. (*A*) Influence of refractive index; curves from left to right were obtained for $n = 1.50$, 1.55, 1.60, and 1.65, respectively, with t and k values as noted in the panel. Insert shows the least-squares fitting error as a function of n, obtained with the optimal value of $k = 0.22$, for different t values: 7.2 nm in curve 1, 6.8 nm in curve 2, and 6.4 nm in curve 3. (*B*) Influence of lipid film average thickness; curves from left to right were obtained for $t = 5.5$ nm, 6.0 nm, 6.5 nm, and 7.0 nm, respectively, with n and k values as noted. Insert shows the least-squares fitting error as a function of t, obtained with the optimal value of $k = 0.22$, for different n values: 1.54 in curve 1, 1.52 in curve 2, and 1.50 in curve 3. (*C*) Influence of nonresonant absorption coefficient; curves from bottom up were obtained for $k = 0.15$, 0.20, 0.25, and 0.30, respectively, with n and t values as noted. Insert shows the least-squares fitting error as a function of k, obtained with the optimal value of $n = 1.52$ for different t values: 7.2 nm in curve 1, 6.8 nm in curve 2, and 6.4 nm in curve 3.

that the SPR method can be effectively used to study structural changes occurring in proteolipid layers deposited on a metallic film (Salamon et al., 1994a,b), as well as to determine the binding affinities of various interacting biological materials (Salamon et al., 1995; Soulages et al., 1995).

In the present implementation of this methodology, a theoretical fit is initially obtained to the SPR spectrum of the bare metal film in contact with aqueous buffer (see below for additional description of the metal/water interface). This enables one to determine the thickness and other optical parameters of the silver film. Next, the SPR spectrum obtained after a lipid layer is deposited onto the metal surface (Salamon et al., 1994b) can similarly be fit with a theoretical curve. The parameters obtained for the uncoated metal are used in the fitting procedure, assuming a two-layered system consisting of the metallic film plus a lipid/water film, each having characteristic n, k, and t values (cf. Eq. 2). Incorporation of a protein such as rhodopsin into the bilayer generates a new SPR spectrum, which is again analyzed by application of a multilayer model, utilizing the uncoated metal parameters and a parameter set characterizing the proteolipid layer (i.e., comprising PC/rhodopsin/water). Finally, in fitting the SPR spectra obtained after the addition of G_t, it is assumed that the latter protein binds to form a separate layer at the proteolipid-water interface. The fitting procedure then utilizes the parameter sets obtained previously for the metal and proteolipid phases to calculate the parameters of the transducin layer in terms of a multilayer model. In previous implementations of this procedure to the binding of proteins whose crystal structures have been determined [cytochrome *c* (Salamon et al., 1995), photoactive yellow protein (Salamon et al., 1995), and apolipophorin III (Soulages et al., 1995)] to a lipid bilayer, values have been obtained for the dimensions of the adsorbed protein layer that were in good agreement with the x-ray results.

Experimental errors

There are two principal sources of error (Salamon et al., 1994b) associated with the fitting procedure and with the estimation of the mass of deposited material. Random experimental errors originate in the accuracy of the incident angle measurement, in the calibration of the resonance spectrum according to the critical angle for total internal reflection, and in uncertainties arising from the signal-to-noise characteristics of the SPR spectrum. The largest random error in the absolute values of the optical parameters obtained from the SPR spectra derives from variations in the reproducibility of the lipid bilayer membrane, which in turn depends on the metallic surface, the parameters of the lipid bilayer membrane-forming solution [i.e., lipid concentration (Salamon et al., 1994b) and the composition of the lipid solvent (Plant, 1993)], and the temperature. Such random variations are estimated to lead to the following uncertainties in the optical parameter values: $n = \pm 0.02$, $t = \pm 1$ Å, and $k = \pm 0.02$. All error limits reported below refer to such random error estimates.

Systematic errors are primarily due to the assumptions made in the choice of structural models for data reduction and analysis, which is particularly important in the case of complex materials such as proteolipid films. The influence of such systematic errors is more difficult to deal with. In terms of the modeling of the metallic film and the deposited dielectric layer(s), there are two problems that arise. First, one must decide whether to treat the deposited dielectric as a multilayer or as a single layer containing a mixture of materials (if a multilayer is chosen, it is necessary in the fitting procedure to assume that the parameters of the first layer are not altered by binding of the second layer; although it is difficult to assign a value to the error introduced by this assumption, it is probably relatively small). In the present case, we have assumed (as noted above) that the rhodopsin-PC film can be considered as a single layer and that the adsorbed transducin comprises an additional separate layer. Although this seems quite reasonable as a first approximation, ultimately the justification for the use of such a model lies in the fact that it yields values for n and t that are consistent with the known structural features of the molecules involved (see below).

The second problem to be noted is as follows. In the mass calculation using the Lorentz-Lorenz relationship, we generally assume that the fully packed layer (under saturation conditions) is completely free of buffer. As noted previously (Salamon et al., 1994b), the Lorentz-Lorenz relation can be applied to two different situations: 1) dilute films that include a contribution from the solvent (having n values of approximately 1.5 or smaller); and 2) films of pure solvent-free lipid and/or protein (having n values larger than 1.5). In the dilute film case, the appropriate equation for the deposited mass, m, is the following:

$$m = 0.3\, t f(n)\, (n - n_s)/ \\ [D/M - V(n_s^2 - 1)/(n_s^2 + 2)] \quad (4)$$

where $f(n) = (n + n_s)/[(n^2 + 2)(n_s^2 + 2)]$, n_s is the refractive index of solvent, D is the molar refractivity of the layer of material, M is the molar mass of the layered substance, V is the partial specific volume of the material, t is the thickness of the layer, and n is the refractive index of the layer. The latter situation with pure lipid and/or protein can be described by the following simpler equation, which does not involve solvent parameters:

$$m = 0.1\, t\, (M/D)\, [(n^2 - 1)\, /(n^2 + 2)] \quad (5)$$

It should be noted that both of these relationships are approximations to the real situation. In the present application, we use the simpler Eq. 5 for mass calculations in the range of concentrations where the SPR spectral changes are saturated, and the more complex Eq. 4 below the saturation range. Yet another approach to mass calculations (useful for simple situations when k is close to zero) is to use the shift in incident angle ($\Delta\alpha$) as a direct measure of adsorbed mass (this requires a calibration of the mass sensitivity of the SPR apparatus, defined as mass per unit surface area per unit angle shift; Salamon et al., 1994a). Assuming the largest experimental errors in the optical parameters, we estimate that the resulting mass errors are approximately $\pm 10\%$.

There are three additional experimental factors that can influence the mass calculation. The first of these results from the incorporation of lipid solvent into the bilayer membrane, which is known to cause changes in the thickness and dielectric constant of freely suspended lipid films (Benz et al., 1975; Plant, 1993). In SPR experiments in our laboratory, it has been observed that increasing the squalene concentration in the solvent mixture with butanol from 2% to 5% causes an increase in both t (~9%) and n (~4%), resulting in an increase of ~11% in the calculated mass. The second factor relates to the formation of a thin layer (3–8 Å) of hydrated oxide on the surface of a silver film in contact with water (Pockrand et al., 1977). This will cause an increase in the apparent thickness of the deposited lipid layer, as well as in the calculated mass. The third factor involves the detailed structure of the surface of the silver film, especially the roughness of the surface and thus the actual physical surface area. This could also cause an increase in the calculated mass per unit area. Inasmuch as these last two factors are variable quantities, it is difficult to estimate the amount of error they introduce into a given experiment. Under the conditions of the rhodopsin experiments to be described below (i.e., films made from solutions containing 7 mg/ml PC and 0.2:10 v/v squalene/butanol), using the model outlined above in conjunction with Eq. 5, we calculate typical average values for the thickness and refractive index of the lipid films of 6.6 nm and 1.54, respectively, which correspond to an area per PC molecule in the range of 50 Å^2 (cf. Salamon et al., 1994b, for a comparison). This value for the area is somewhat smaller than expected for liquid crystalline bilayers (Thurmond et al., 1991), which may reflect the neglect of surface roughness in the calculations.

RESULTS AND DISCUSSION

Characterization of rhodopsin-containing membrane films and influences of light

Typical SPR spectra obtained in the dark (before illumination of the sample) are presented in Fig. 3. Curve 1 is the resonance spectrum for a bare silver film in contact with buffer solution, curve 2 is obtained after deposition of an egg PC bilayer, and curve 3 shows the spectrum after the addition of a saturating amount of rhodopsin. As reported previously (Salamon et al., 1994a), the incorporation of rhodopsin into the PC film shifts the SPR spectrum to larger angles (due to increases in n and t; cf. Fig. 2), causes a large increase in the resonance depth (due to an increase in n and a decrease in k; cf. Fig. 2), and decreases the half-width of the curve (due to an increase in t and a decrease in k; cf. Fig. 2). Table 1 gives the calculated parameters obtained from a theoretical fit to the PC/rhodopsin spectrum (shown for

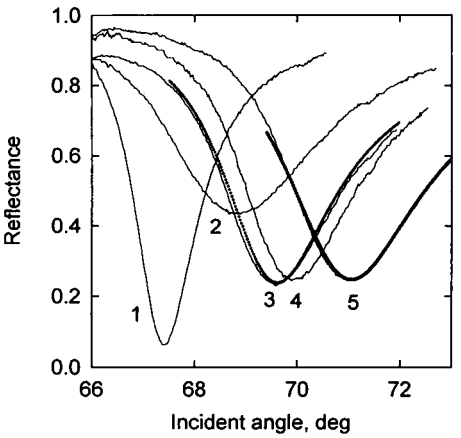

FIGURE 3 SPR spectra obtained with a silver film of 52 nm average thickness and dielectric layers as indicated; the buffer solution in contact with the film contained 10 mM sodium phosphate and 5 mM Mg acetate at pH 6.0 ($T = 23 \pm 1$°C). Reflectance values measure the fractional decrease in the total reflected light. (*Curve 1*) Bare metal film in contact with buffer solution. (*Curve 2*) Metal coated with a lipid (PC) bilayer membrane made from a solution containing 7 mg/ml PC in squalene/butanol (2:100, v/v). (*Curve 3*) After the addition of a saturating amount of rhodopsin (total of 7 μM added to the aqueous phase; dotted curve represents a theoretical fit). (*Curves 4,5*) After two incremental additions of G_t to the aqueous compartment (final total concentrations added to the aqueous phase of 40 and 160 nM, respectively; dotted curve represents a theoretical fit to curve 5).

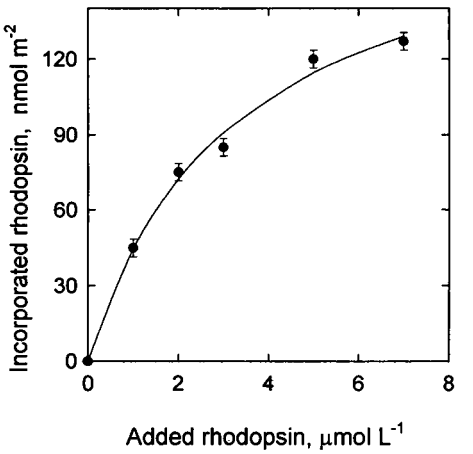

FIGURE 4 Dependence of the surface coverage due to rhodopsin incorporated into a PC bilayer membrane on the protein concentration in the aqueous compartment of the SPR cell, before illumination of the sample. Approximately 0.1% of the total rhodopsin is incorporated at the highest added concentration. All other conditions are as in Fig. 3. Error bars are based on estimated uncertainties in n and t parameters (see text). Solid curve shows a nonlinear least-squares fit to a hyperbolic function; this yields an apparent binding constant of 3.2 μM and a limiting value of 188 nmol m^{-2} rhodopsin incorporated at infinite concentration of added rhodopsin.

curve 3). These values are in good agreement with previous results (Salamon et al., 1994a). Curves 4 and 5 in Fig. 3 were obtained after the addition of G_t and will be discussed below.

Fig. 4 shows a plot of the mass of rhodopsin incorporated into the PC bilayer (calculated using the Lorentz-Lorenz relationships, as described above) as a function of the total concentration of the protein added to the aqueous compartment. From these data, it is clear that incorporation is essentially complete at approximately 5 μM rhodopsin (a least-squares fit to the data, assuming a single hyperbolic binding process according to the Langmuir equation, is shown by the solid curve in Fig. 4; this yields an apparent binding constant of 3.2 μM). We calculate that the incorporation efficiency under the conditions used was approximately 0.1%, which is relatively small. Presumably, the unincorporated rhodopsin remained dispersed in the SPR cell and thus did not give rise to an SPR signal (Salamon et al., 1994a). The hyperbolic fit yields a limiting value of 188 nmol m^{-2} for the surface concentration of rhodopsin incorporated into the lipid membrane at infinite concentration of added rhodopsin. From this value one can calculate an average surface area of 1260 $Å^2$ occupied by a rhodopsin molecule. This is in agreement with the rhodopsin dimensions determined recently by electron cryomicroscopy (~1000 $Å^2$; Schertler et al., 1993; Unger and Schertler, 1995) and from a rhodopsin Langmuir-Blodgett film by x-ray scattering (~1100 $Å^2$; Maxia et al., 1995).

TABLE 1 Calculated SPR parameters for proteolipid (PC/rhodopsin) and transducin layers deposited sequentially on a silver film before illumination*

Layer#	t (Å)	n	k
PC/rhodopsin	87 ± 1	1.62 ± 0.02	0.07 ± 0.02
Transducin	57 ± 1	1.57 ± 0.02	0.00 ± 0.02

*t, thickness; n, refractive index; k, absorption coefficient.
#A multilayer model is assumed; error limits include only influences of random errors (see text for discussion).

The effects of light irradiation on the PC/rhodopsin SPR curve are shown in Fig. 5 *A*. As previously demonstrated (Salamon et al., 1994a), yellow light causes a shift of the SPR spectrum to slightly larger incident angles, without a measurable change in spectral width. We have interpreted this (Salamon et al., 1994a) to be a consequence of MII formation. Inasmuch as MII has been reported to have a lifetime of minutes (cf. Arnis and Hofmann, 1993), and the SPR spectrum is obtained within 1–2 min after irradiation, this assignment is not unreasonable. The data indicate a small increase in average film thickness t, with little or no change in n or k. Also shown in Fig. 5 *A* is the effect of blue light irradiation, which can be seen to shift the SPR spectrum almost back to its original position. Absorption of a second photon of blue light is known to convert MII into a mixture of rhodopsin (11-*cis*-retinal) and isorhodopsin (9-*cis*-retinal). Thus the observed blue light-induced back reaction is additional supporting evidence that the SPR changes upon photolysis of rhodopsin largely manifest the formation of the key MII intermediate in the visual process.

The results shown in the experiments of Fig. 5 *A* clearly indicate that rhodopsin which has been incorporated into a supported PC bilayer retains its photoactivity. To further probe the characteristics of the incorporated rhodopsin, a

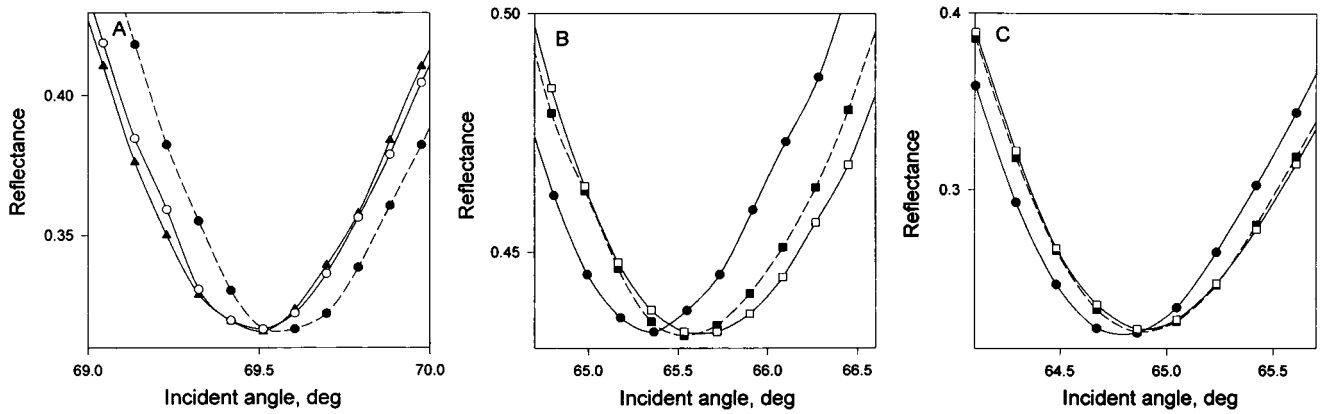

FIGURE 5 (*A*) Effect of light irradiation on the PC/rhodopsin SPR curve. ▲, SPR spectrum obtained before irradiation with a 54-nm-thick silver film coated with a lipid bilayer membrane formed from 10 mg/ml PC in squalene/butanol (5:100, v/v), containing a saturating amount of rhodopsin (total concentration in the aqueous phase was 7 μM), in contact with 5 mM sodium phosphate buffer (pH 5.5). ●, SPR spectrum obtained after irradiation of sample with saturating flashes of yellow light (10 flashes delivered within 1 min); the SPR cell was illuminated from the back through a fiber optic light guide using a Sunpak AP-52 flash unit, fitted with a Schott OG 515 filter ($\lambda > 515$ nm). ○, SPR spectrum after irradiation of the photolyzed sample with saturating flashes of blue light ($\lambda = 300-430$ nm). (*B*) Regeneration of the photolyzed rhodopsin with 11-*cis*-retinal. The SPR spectra were obtained with a 52.5-nm-thick silver film coated with a lipid membrane formed from 10 mg/ml PC in squalene/butanol (4:100, v/v) containing a saturating amount of rhodopsin (total concentration in the aqueous phase was 10 μM), in contact with 5 mM phosphate buffer (pH 5.5). ●, SPR spectrum obtained after saturating flashes of yellow light; conditions as in *A*. ■, SPR spectrum obtained after the addition of 10-fold molar excess of 11-*cis*-retinal in octyl glucoside to the aqueous compartment of the SPR cell. □, SPR spectrum obtained after reirradiation of the sample with yellow light, as in *A*. (*C*) Control experiment performed without rhodopsin present in the lipid bilayer membrane. Symbols and conditions as in *B*.

control regeneration experiment was carried out using an octyl glucoside solution of 11-*cis*-retinal, which was added to the aqueous compartment of the SPR cell after yellow light irradiation of the rhodopsin-containing sample. The results are shown in Fig. 5 *B*. These findings demonstrate clearly that: 1) the addition of a 10-fold molar excess of 11-*cis*-retinal to the aqueous compartment of the SPR cell after rhodopsin photolysis causes small changes in the SPR spectrum, which are similar to those observed upon incorporation of the rhodopsin into the lipid membrane in the dark (see Fig. 3); we interpret these to be due to both specific and nonspecific incorporation of retinal into the lipid layer, thereby increasing its mass (see below); 2) most significantly, the ability of yellow light illumination to cause a shift in the SPR spectrum is restored (compare with Fig. 5 *A*). Moreover, an additional control experiment (Fig. 5 *C*), performed under the same conditions as in Fig. 5 *B*, but without rhodopsin in the lipid film, demonstrates that similar SPR changes occur after addition of retinal to the aqueous solution (associated with nonspecific incorporation of retinal into the lipid film), but without any measurable alterations after yellow light illumination. We conclude from these data that the angular shift caused by nonspecific binding of retinal masks the smaller shift in the opposite direction caused by rhodopsin regeneration. Using a multilayer model, the optical parameters obtained upon fitting the SPR curves in both experiments can be interpreted by an increase of the proteolipid membrane thickness in the range of 5–8 Å, without an appreciable change in n, upon the addition of 11-*cis*-retinal. This result in turn implies a proteolipid mass increase of 6–9%, indicating a quite efficient incorporation of 11-*cis*-retinal into the lipid membrane interior. The ratio of the angular shift caused by yellow light after regeneration (Fig. 5 *B*) to that before regeneration (Fig. 5 *A*) is about 0.7, which suggests that about 70% of rhodopsin was regenerated.

Transducin binding to rhodopsin as detected by SPR spectroscopy

Returning now to Fig. 3, curves 4 and 5 illustrate SPR spectra obtained after two incremental additions of a G_t solution in buffer to the aqueous compartment. As can be seen, G_t binding causes a large increase in the incident angle at the resonance minimum, and a small increase in the spectral width, without any change in the resonance depth. These changes are consistent with an increase in both n and t, but without much change in k. The SPR data clearly indicate that G_t molecules adsorb to the PC-rhodopsin membrane in the dark, leading to the formation of an additional layer of bound protein. By fitting the experimental SPR curves using the theoretical model described above (shown for curve 5 in Fig. 3), the optical parameters that describe the adsorbed G_t can be evaluated in terms of a multilayer model (Table 1). The analysis suggests that the G_t region has an average thickness of 5.7 nm (total calculated proteolipid/G_t film thickness is 14.4 nm), which is consistent with the dimensions of the roughly ellipsoidal G_t α-subunit as determined by x-ray crystallography (dimensions approximately 4.8 × 6.2 nm, based on the crystallographic structure; Noel et al., 1993; Coleman et al., 1994). In addition, the value of the refractive index of the protein layer indicates a relatively high surface packing density of G_t (see below). It is important to note that a control experiment

using a PC bilayer membrane without rhodopsin at pH 6.0 revealed no detectable SPR spectral changes upon G_t addition (data not shown), demonstrating that no interaction occurred between the pure PC membrane and the G_t molecules under these conditions.

As noted in the Introduction, it is generally accepted that G_t is a peripheral protein that associates with the ROS membrane; as yet there is no comprehensive understanding of these associations. Several lines of evidence suggest that membrane attachment is partly due to lipid modifications of the α- and γ-subunits (Bigay et al., 1994; Matsuda et al., 1994); other evidence points to rhodopsin as providing the main docking site for G_t (Inglese et al., 1992; Dratz et al., 1993; Conklin et al., 1993). Although the present SPR results also implicate rhodopsin in G_t binding before illumination, we cannot rule out the possibility of a much weaker interaction with the PC bilayer. Such weak binding is suggested by the results of Matsuda et al. (1994), in which the molar ratio of G_t to PC in vesicles was determined to be approximately $1:10^4$. However, this is below the present level of detection by SPR.

The optical parameters can also be used to calculate the mass of the adsorbed molecules using the above-mentioned Lorentz-Lorenz formalism. In Fig. 6, the data obtained at various levels of protein addition are plotted in terms of the increase of mass due to the adsorption of G_t onto the membrane. From these results, several important conclusions can be drawn. First, the binding constant of G_t to unactivated rhodopsin is approximately 60 nM, which is consistent with the highest affinities that have been reported for binding to dark-adapted rhodopsin (Hamm et al., 1987; Schleicher and Hofmann, 1987). However, the binding is still significantly weaker than the largest values found for light-activated rhodopsin (Bennett and Dupont, 1985; König et al., 1989). Second, a value of approximately 2000

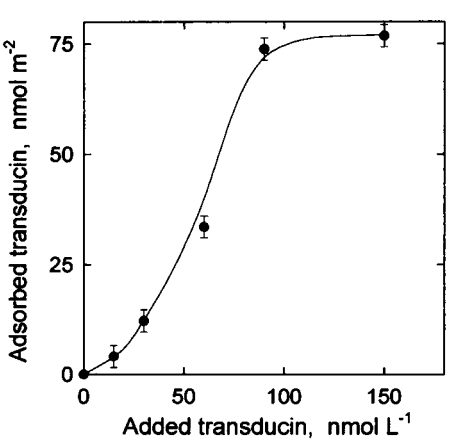

FIGURE 6 Dependence of the surface coverage due to transducin bound to a PC/rhodopsin bilayer membrane on the protein concentration in the aqueous compartment of the SPR cell before illlumination of the sample. Note that the bulk concentration scale is smaller than in Fig. 4. The surface coverage by rhodopsin was approximately 100 nmol m^{-2}; all other conditions were as in Fig. 3. Error bars are based on uncertainties in n and t parameters.

Å^2 for the surface area per molecule of G_t (at saturation) can be estimated from the data presented in Fig. 6; this is also broadly consistent with the dimensions of the x-ray structure and suggests a relatively high surface packing density of G_t. Third, the sigmoidal shape of the binding curve suggests positive cooperativity in the binding of G_t to dark-adapted rhodopsin, whereas the incorporation of rhodopsin into the bilayer occurs in an apparently noncooperative manner (Fig. 4). Although previous studies (Wessling-Resnick and Johnson, 1987; König et al., 1989) have indicated positively cooperative interactions between MII and G_t, to our knowledge this is the first indication of such cooperativity in the interaction between G_t and rhodopsin during the stages before the activation of the receptor.

It is noteworthy that the calculated values for the molar ratio of G_t to rhodopsin were in the range of 0.6 ± 0.1 at saturating concentrations of both proteins, which implies a stoichiometry of less than 1:1. If so, this could be a consequence of two factors: 1) the larger size of G_t relative to rhodopsin, which would preclude total ligation in a close-packed membrane; and 2) the possibility that not all of the rhodopsin is incorporated into the bilayer with the G_t binding domain facing the aqueous compartment. The transducin/rhodopsin molar ratio calculated here can be compared to a value of 0.2–0.25 reported for the ROS membrane (Baehr et al., 1982). Although further work is required to determine the reasons for this apparent disparity, it is possible that the higher rhodopsin concentrations calculated for the present system may lead to more effective G_t binding via cooperativity.

Effects of illumination and addition of GTP on the SPR spectra of PC/rhodopsin/transducin films

After reaching saturation of the binding of G_t to rhodopsin (150 nM of added G_t; cf. Fig. 6), the sample was illuminated by 10 sequential flashes of yellow light ($\lambda > 515$ nm), which were sufficient to saturate the SPR changes. As shown previously (Gibson and Brown, 1993; Salamon et al., 1994a), these convert rhodopsin to the MII form. SPR spectra were measured, and a small aliquot of a concentrated solution of GTP in aqueous buffer was added to the sample (final concentration 100 μM). In Fig. 7, typical SPR curves are presented, using curve 5 of Fig. 3 *A* plotted on an expanded incident angle scale (Fig. 7, curve 1) to illustrate the light effect (shown in curve 2) and the GTP effect (shown in curve 3). The shifts of the resonance minimum to larger incident angles (due to increases in n and/or t) caused by these additions is clearly apparent, as is the alteration in the spectral shape (broadening and decrease in reflectance, suggesting an increase in k) caused by the addition of GTP (curve 3).

To interpret the light-induced SPR spectral modifications shown in Fig. 7, in the context of the three-layer model noted above (i.e., silver, proteolipid, and G_t regions), one can assume that the spectral changes are due either to conformational alterations of rhodopsin accompanying for-

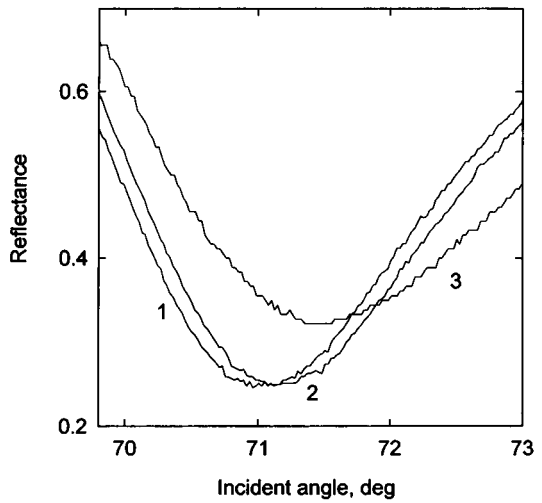

FIGURE 7 Effect of illumination with yellow light and of GTP addition on SPR spectra of PC/rhodopsin/transducin film. (*Curve 1*) Corresponds to curve 5 from Fig. 3. (*Curve 2*) Obtained after saturating flashes of yellow light (10 flashes delivered within 1 min); the SPR cell was illuminated from the back through a fiber optic light guide using a Sunpak AP-52 flash unit, fitted with a Schott OG 515 filter (wavelength > 515 nm, which converts rhodopsin to MII). (*Curve 3*) Obtained after the addition of 100 μM (final concentration) GTP to the aqueous compartment.

mation of the MII state, or to processes accompanying the interaction between G_t and photolyzed rhodopsin, or to both. First, it should be noted that the SPR spectra obtained after irradiation can be fit by increasing the average thickness of either the PC/rhodopsin or the G_t layers by approximately 6 Å, without any significant change in n. This can be compared with an average thickness change of approximately 2.5 Å previously obtained upon light irradiation in the absence of G_t, again without any detectable change in n, which was interpreted as representing the formation of MII (Salamon et al., 1994a). An interesting question is whether the larger SPR change currently observed after G_t addition implies that there is a light-induced increase in the amount of G_t bound to the rhodopsin-containing membrane. There are two experimental indications that argue against this interpretation. First, the absence of a detectable change in the refractive index of the G_t layer upon photolysis suggests that the density of the adsorbed protein layer is not changing appreciably. Second, as noted above, the dark rhodopsin-G_t interaction apparently results in a closely packed G_t layer, suggesting that there is little or no free space in the protein layer to incorporate more molecules (i.e., binding is already saturated). Therefore, an increase in the affinity of G_t to rhodopsin caused by MII formation would not be expected to yield a change in the number of molecules bound. According to this view, the "extra thickness" of the system could originate either from conformational changes of the G_t molecules resulting from the MII-G_t binding, or from generation of extra MII upon binding of transducin (Hofmann, 1986; König et al., 1989; Franke et al., 1990), or both. These tentative conclusions require further study.

Finally, the addition of 100 μM GTP to the aqueous phase of the sample compartment causes further interesting changes in the SPR spectrum (see curve 3, Fig. 7). These changes, which we interpret to be due to alterations in the G_t layer, result in an increase in the calculated value of n (by 0.05) and only a small change in t (by about 1 Å, which is close to our experimental uncertainty). There is also a significant increase in the k parameter (by 0.05), possibly indicating an alteration in the surface roughness of the protein layer, which causes more evanescent wave scattering and concomitantly a loss in reflected intensity. The increase in the refractive index may suggest that after the addition of GTP, the G_t layer becomes more densely, although less regularly, packed with protein material. Such results can be ascribed to one or more of several processes (Dratz et al., 1993; Noel et al., 1993; Coleman et al., 1994): 1) changes in the conformation of G_t due to GTP binding; 2) binding of GTP to the empty nucleotide binding pocket (although because of the small mass involved, this should only result in relatively small SPR changes); 3) dissociation of the G_t α-subunit from MII; and 4) formation of new G_t-MII complexes, which may result in a more irregularly packed protein layer. Although the present steady-state SPR measurements cannot distinguish among these different phenomena, it may be possible to accomplish this in the future with time-resolved experiments.

CONCLUSIONS

The above results clearly demonstrate the utility of SPR spectroscopy as a tool for the study of the biochemistry of membrane receptors, for which rhodopsin is an important paradigm. Such SPR measurements may find eventual practical implementation in biosensors. In this regard, studies of signal transduction in the visual system constitute an important step. The present work confirms and extends our knowledge of the interactions between rhodopsin and transducin in a particularly direct manner. Quantitative measurements of the binding cooperativity, affinity, and stoichiometry involving these two proteins, before conversion of rhodopsin to the MII state, have been achieved in thin membrane films on a planar metal substrate. The data also indicate that the application of time-resolved SPR spectroscopy to this system may enable further insights to be obtained into the time course of the structural events occurring within a rhodopsin/G_t complex, after activation of rhodopsin by light and the resulting exchange of GDP by GTP. These and related studies have the potential of opening up a new avenue for molecular-level dissection of the interactions among proteins associated with membranes. Moreover, such investigations provide vital new information regarding the biochemistry and biophysics of signal transduction systems in general.

This work was supported by grants from the Vice President for Research at the University of Arizona (to ZS and GT) and the National Science

Foundation (MCB-9404702; to ZS and GT), and by National Institutes of Health grants EY03754 and EY10622 (to MFB).

REFERENCES

Arnis, S., and K. P. Hofmann. 1993. Two different forms of metarhodopsin II: Schiff base deprotonation precedes proton uptake and signaling state. *Proc. Natl. Acad. Sci. USA.* 90:7849–7853.

Arnis, S., and K. P. Hofmann. 1995. Photoregeneration of bovine rhodopsin from its signaling state. *Biochemistry.* 34:9333–9340.

Baehr, W., E. A. Morita, R. J. Swanson, and M. L. Applebury. 1982. Characterization of bovine rod outer segment G-protein. *J. Biol. Chem.* 257:6452–6460.

Bennett, N., and Y. Dupont. 1985. The G-protein of retinal rod outer segments (transducin). *J. Biol. Chem.* 260:4156–4168.

Benz, R., O. Fröhlich, P. Lauger, and M. Montal. 1975. Electrical capacity of black lipid films and of bilayers made from monolayers. *Biochim. Biophys. Acta.* 394:323–334.

Bigay, J., E. Faurobert, M. Franco, and M. Chabre. 1994. Roles of lipid modifications of transducin subunits in their GDP-dependent association and membrane binding. *Biochemistry.* 33:14081–14090.

Born, M., and E. Wolf. 1965. Principles of Optics. Pergamon Press, New York.

Bourne, H. R., D. A. Sanders, and F. McCormick. 1990. The GTPase superfamily: a conserved switch for diverse cell functions. *Nature.* 348:125–132.

Bourne, H. R., D. A. Sanders, and F. McCormick. 1991. The GTPase superfamily: conserved structure and molecular mechanism. *Nature.* 349:117–123.

Brown, M. F. 1994. Modulation of rhodopsin function by properties of the membrane bilayer. *Chem. Phys. Lipids.* 73:159–180.

Coleman, D. E., A. M. Berghuis, E. Lee, M. E. Linder, A. G. Gilman, and S. R. Sprang. 1994. Structures of active conformations of $G_{i\alpha 1}$ and the mechanism of GTP hydrolysis. *Science.* 265:1405–1412.

Conklin, B. R., Z. Farfel, K. D. Lustig, D. Julius, and H. R. Bourne. 1993. Substitution of three amino acids switches receptor specificity of $G_q\alpha$ to that of $G_i\alpha$. *Nature.* 363:274–276.

Corless, J. M., D. R. McCaslin, and B. L. Scott. 1982. Two-dimensional rhodopsin crystals from disk membranes of frog retinal ROS. *Proc. Natl. Acad. Sci. USA.* 79:1116–1120.

Corson, D. W., M. C. Cornwall, E. F. MacNichol, J. Jin, R. Johnson, F. Derguini, R. K. Crouch, and K. Nakanishi. 1990. Sensitization of bleached rod photoreceptors by 11-cis-locked analogues of retinal. *Proc. Natl. Acad. Sci. USA.* 87:6823–6827.

Deese, A. J., E. A. Dratz, and M. F. Brown. 1981. Retinal ROS lipids form bilayers in the presence and absence of rhodopsin. *FEBS Lett.* 124: 93–99.

Dixon, R. A. F., I. S. Sigal, and C. D. Strader. 1988. Structure-function analysis of the β-adrenergic receptor. *Cold Spring Harb. Symp. Quant. Biol.* 53:487–497.

Dratz, E. A., J. E. Furstenau, C. G. Lambert, D. L. Thireault, H. Rarick, T. Schepers, S. Pakhlevaniants, and H. E. Hamm. 1993. NMR structure of a receptor-bound G-protein peptide. *Nature.* 363:276–281.

Emeis, D., H. Kühn, J. Reichert, and K. P. Hofmann. 1982. Complex formation between metarhodopsin II and GTP-binding protein in bovine photoreceptor membranes leads to a shift of the photoproduct equilibrium. *FEBS Lett.* 143:29–34.

Franke, R. R., B. König, T. P. Sakmar, H. G. Khorana, and K. P. Hofmann. 1990. Rhodopsin mutants that bind but fail to activate transducin. *Science.* 250:123–125.

Franke, R. R., T. P. Sakmar, D. D. Oprian, and H. G. Khorana. 1988. A single amino acid substitution in rhodopsin (Lysine 248-leucine) prevents activation of transducin. *J. Biol. Chem.* 263:2119–2122.

Fung, B. K. K. 1983. Characterization of transducin from bovine retinal rod outer segments. *J. Biol. Chem.* 258:10495–10502.

Fung, B. K. K., J. B. Hurley, and L. Stryer. 1981. Flow of information in the light-triggered cyclic nucleotide cascade of vision. *Proc. Natl. Acad. Sci. USA.* 78:152–156.

Gibson, N. J., and M. F. Brown. 1993. Lipid headgroup and acyl chain composition modulate the MI-MII equilibrium of rhodopsin in recombinant membranes. *Biochemistry.* 32:2438–2454.

Gilman, A. G. 1987. G proteins: transducers of receptor-generated signals. *Annu. Rev. Biochem.* 56:615–649.

Haltom, T. L., E. T. Arakawa, M. W. Williams, and E. Kretschmann. 1979. Refractive index of LiF films as a function of time. *Appl. Opt.* 18: 1233–1236.

Hamm, H. E. 1991. Molecular interactions between the photoreceptor G protein and rhodopsin. *Cell. Mol. Neurobiol.* 11:563–578.

Hamm, H. E., D. Deretic, A. Arendt, P. A. Hargrave, B. König, and K. P. Hofmann. 1988. Site of G protein binding to rhodopsin mapped with synthetic peptides from the α subunit. *Science.* 241:832–835.

Hamm, H. E., D. Deretic, K. P. Hofmann, A. Schleicher, and B. Kohl. 1987. Mechanism of action of monoclonal antibodies that block the light activation of the guanyl nucleotide-binding protein, transducin. *J. Biol. Chem.* 262:10831–10838.

Hargrave, P. A., and J. H. McDowell. 1992. Rhodopsin and phototransduction: a model system for G protein-linked receptors. *FASEB J.* 6:2323–2331.

Hausdorff, W. P., M. Hnatowich, B. F. O'Dowd, M. G. Caron, and R. J. Lefkowitz. 1990. A mutation of the β_2-adrenergic receptor impairs agonist activation of adenylyl cyclase without affecting high affinity agonist binding. *J. Biol. Chem.* 265:1388–1393.

Hofmann, K. P. 1986. Photoproducts of rhodopsin in disk membranes. *Photobiochem. Photobiophys.* 13:309–327.

Inglese, J., W. J. Koch, M. G. Caron, and R. J. Lefkowitz. 1992. Isoprenylation in regulation of signal transduction by G-protein-coupled receptor kinases. *Nature.* 359:147–150.

Jones, G. J., R. K. Crouch, B. Wiggert, M. C. Cornwall, and G. J. Chader. 1989. Retinoid requirements for recovery of sensitivity after visual-pigment bleaching in isolated photoreceptors. *Proc. Natl. Acad. Sci. USA.* 86:9606–9610.

Kibelbek, J., D. C. Mitchell, J. M. Beach, and B. J. Litman. 1991. Functional equivalence of metarhodopsin II and the G_t-activating form of photolyzed bovine rhodopsin. *Biochemistry.* 30:6761–6768.

König, B., A. Arendt, J. H. McDowell, M. Kahlert, P. A. Hargrave, and K. P. Hofmann. 1989. Three cytoplasmic loops of rhodopsin interact with transducin. *Proc. Natl. Acad. Sci. USA.* 86:6878–6882.

Kretschmann, E. 1971. Die Bestimmung optischer konstanten von Metallen durch Anregung von Oberflachenplasmaschwingungen. *Z. Phys.* 241:313–324.

Kühn, H. 1980. Light- and GTP-regulated interaction of GTPase and other proteins with bovine photoreceptor membranes. *Nature.* 283:587–589.

Liddell, H. M. 1981. Computer-aided Techniques for the Design of Multilayer Filters. Hilger, Bristol.

Lopez-Rios, T., and G. Vuye. 1979. Use of surface plasmon excitation for determination of the thickness and optical constants of very thin surface layers. *Surf. Sci.* 81:529–538.

Macleod, H. A. 1986. Thin Film Optical Filters. Hilger, Bristol.

Matsuda, T., T. Takao, Y. Shimonishi, M. Murata, T. Asano, T. Yoshizawa, and Y. Fukada. 1994. Characterization of interactions between transducin $\alpha/\beta\gamma$-subunits and lipid membranes. *J. Biol. Chem.* 269: 30358–30363.

Maxia, L., G. Radicchi, I. M. Pepe, and C. Nicolini. 1995. Characterization of Langmuir-Blodgett films of rhodopsin: thermal stability studies. *Biophys. J.* 69:1440–1446.

Michel-Villaz, M., A. Brisson, and Y. Chapron. 1984. Physical analysis of light-scattering changes in bovine photoreceptor membrane suspensions. *Biophys. J.* 46:655–662.

Mueller, P., D. O. Rudin, H. T. Tien, and W. C. Wescott. 1962. Reconstitution of cell membrane structure in vitro and its transformation into an excitable system. *Nature.* 194:979–980.

Noel, J. P., H. E. Hamm, and P. B. Sigler. 1993. The 2.2 Å crystal structure of transducin-α complex with GTPγS. *Nature.* 366:654–663.

Papermaster, D. S., and W. J. Dreyer. 1974. Rhodopsin content in the outer segment membranes of bovine and frog retinal rods. *Biochemistry.* 13:2438–2444.

Plant, A. L. 1993. Self-assembled phospholipid/alkanethiol biomimetic bilayers on gold. *Langmuir.* 9:2764–2767.

Pockrand, I., J. D. Swalen, J. G. Gordon, and M. R. Philpott. 1977. Surface plasmon spectroscopy of organic monolayer assemblies. *Surf. Sci.* 74: 237–244.

Salamon, Z., T. E. Meyer, and G. Tollin. 1995. Photobleaching of the photoactive yellow protein from *Ectothiorhodospira halophila* promotes binding to lipid bilayers: evidence from surface plasmon resonance spectroscopy. *Biophys. J.* 68:648–654.

Salamon, Z., Y. Wang, M. F. Brown, H. A. Macleod, and G. Tollin. 1994a. Conformational changes in rhodopsin probed by surface plasmon resonance spectroscopy. *Biochemistry.* 33:13706–13711.

Salamon, Z., Y. Wang, G. Tollin, and H. A. Macleod. 1994b. Assembly and molecular organization of self-assembled lipid bilayers on solid substrates monitored by surface plasmon resonance spectroscopy. *Biochim. Biophys. Acta.* 1195:267–275.

Schertler, G. F. X., C. Villa, and R. Henderson. 1993. Projection structure of rhodopsin. *Nature.* 362:770–772.

Schleicher, A., and K. P. Hofmann. 1987. Kinetic study on the equilibrium between membrane bound and free photoreceptor G-protein. *J. Membr. Biol.* 95:271–281.

Schulz, L. G., and F. R. Tangherlini. 1954. Optical constants of silver, gold, and aluminum. II. The index of refraction *n*. *J. Opt. Soc. Am.* 44:362–368.

Simon, M. L., M. P. Strathmann, and N. Gautman. 1991. Diversity of G proteins in signal transduction. *Science.* 252:802–808.

Soulages, J. L., Z. Salamon, M. A. Wells, and G. Tollin. 1995. Low concentrations of diacylglycerol promote the binding of apolipophorin III to a phospholipid bilayer: a surface plasmon resonance spectroscopy study. *Proc. Natl. Acad. Sci. USA.* 92:5650–5654.

Stryer, L. 1991. Visual excitation and recovery. *J. Biol. Chem.* 266: 10711–10714.

Sukumar, M., and T. Higashijma. 1992. G protein-bound conformation of mastoparan-X, a receptor-mimetic peptide. *J. Biol. Chem.* 267: 21421–21424.

Sullivan, K. A., R. T. Miller, S. B. Masters, B. Beiderman, W. Heideman, and H. R. Bourne. 1987. Identification of receptor contact site involved in receptor-G-protein coupling. *Nature.* 330:758–760.

Surya, A., K. W. Foster, and B. E. Knox. 1994. Transducin activation by the bovine opsin apoprotein. *J. Biol. Chem.* 270:5024–5031.

Tang, J. F., and Q. Zheng. 1982. Automatic design of optical thin-film systems: merit function and numerical optimization method. *J. Opt. Soc. Am.* 72:1522–1528.

Taylor, C. W. 1990. The role of G proteins in transmembrane signaling. *Biochem. J.* 272:1–13.

Thurmond, R. L., S. W. Dodd, and M. F. Brown. 1991. Molecular areas of phospholipids as determined by ^{2}H NMR spectroscopy. *Biophys. J.* 59:108–113.

Unger, V. M., and G. F. X. Schertler. 1995. Low resolution structure of bovine rhodopsin determined by electron cryo-microscopy. *Biophys. J.* 68:1776–1786.

Weingarten, R., L. Rosnas, H. Mueller, L. A. Sklar, and G. M. Bokoch. 1990. Mastoparan interacts with the carboxyl terminus of the α subunit of G_i. *J. Biol. Chem.* 265:11044–11052.

Wessling-Resnick, M., and G. L. Johnson. 1987. Allosteric behavior in transducin activation mediated by rhodopsin. *J. Biol. Chem.* 262: 3697–3705.

Wiedmann, T. S., R. D. Pates, J. M. Beach, A. Salmon, and M. F. Brown. 1988. Lipid-protein interactions mediate the photochemical function of rhodopsin. *Biochemistry.* 27:6469–6474.

Wilden, U., and H. Kühn. 1982. Light-dependent phosphorylation of rhodopsin: number of phosphorylation sites. *Biochemistry.* 21: 3014–3022.

Zhang, F. S., R. W. Wang, H. A. Macleod, R. E. Parks, and R. E. Jacobson. 1987. Surface plasmon detection of surface contamination of metallic film surfaces. *Proc. Soc. Photo-Opt. Instrum. Eng.* 777:163–170.